

ITB Formation During Slow Electron and Ion Heat Pulse Propagation in Tokamaks

S. V. Neudatchin 1) , D. A. Shelukhin, 1)

1) Institute Tokamak Physics, RRC Kurchatov Institute, Russia, Moscow,123182, Kurchatov sq 1

E-mail: neudatchin@nfi.kiae.ru

Abstract Understanding of properties of internal transport barrier (ITB) is of importance for the fusion research of toroidal magnetic confinement. In T-10, ITB has been recognized by means of analyses of heat pulse propagation (HPP) induced by central ECRH-onset and cold pulse propagation (CPP) by off-axis ECRH cut-off in a sawtooth-free plasma created by off-axis ECRH. The cold pulses propagate slowly and diffusively with dynamic electron heat diffusivity $\chi_e^{HP} \sim 0.1 \text{ m}^2/\text{s}$. It has been known for many years, that in L-mode, $\chi_e^{HP} \approx 2-4 \chi_e^{PB}$ (so called “enhanced” HPP). At present, this relationship is usually explained by “critical gradient model”. In the present report, we focus on the fully opposite cases with $\chi_e^{HP} < \chi_e^{PB}$. For the first time, this case was found at T-10 in 1990 and called “self-deceleration of heat wave”, or, in contrast with L-mode, “reduced” or “slow” HPP. Non-local confinement bifurcations (jump of core transport at $\sim 0.3-0.4r/a$ region inside and around ITB in a ms timescale) were found in various JT-60U normal and RS plasmas and called ITB-events. Later, ITB-events were found in T-10 plasmas. At the same time, HPP is diffusive between the non-local bifurcations of the transport. Slow outward electron and ion HPP ($\chi_{e,i}^{HP} \sim 0.1 \text{ m}^2/\text{s} \ll \chi_{e,i}$) induced by ITB-event was observed in JT-60U. The new method allows reconstructing a gradual reduction of $\chi_{e,i}(r,t)$ during slow electron and ion HPP in the situations described above. The values of $\chi_{e,i}$ remain higher compare with $\chi_{e,i}^{HP}$ values. In T-10, the dynamic of ITB formation is similar with ECRH at first harmonic (1990) and the second one. In T-10, the reconstructed decay of χ_e fits well the value of χ_e at the end of CPP (obtained independently from the power balance). level The of fluctuations measured by reflectometer falls below the Ohmic level in shots with slow CPP in T-10. In J-60U, the gradual decay of $\chi_{e,i}$ during HPP is accompanied by the rise of the radial electric field E_r shear calculated with neoclassical velocity of the poloidal rotation. In contrast to this, E_r just begins to vary slowly after ITB-event.

1. Introduction

The value measured by various analytical and numerical methods of HPP analysis is not the power balance electron heat diffusivity χ_e^{PB} value (obtained from electron heat flux derived from transport code calculations) but $\chi_e^{HP} = \delta\Gamma_e / (n_e \delta\nabla T_e)$, where χ_e^{HP} is dynamic electron heat diffusivity, $\delta\Gamma_e$ is electron thermal flux perturbation and $\delta\nabla T_e$ is ∇T_e perturbation. With regards to the perturbations of the heat sources and density (normalised variation of density is much lower compare with that of for T_e in the experiments reported below), HPP/CPP is usually analysed using a simplified transport equation for δT_e , (see e.g. [1-4]):

$$1.5n_e \partial\delta T_e / \partial t = \text{div}(n_e \chi_e^{HP} \nabla\delta T_e) \quad (1)$$

An important experimentally measured characteristic of the CPP is the index of the relative sharpness of a heat wave (Sh) (see [4-6]):

$$\text{Sh} = |(\delta\nabla T_e / \delta T_e) / (\nabla T_{e0} / T_{e0})|. \quad (2)$$

The value of Sh characterizes the sensitivity of the diffusive term ($\chi_e^{HP} \delta\nabla T_e$) to the terms proportional to δT_e such as convective and convective-like terms (electron-ion exchange sources perturbations, dependence of χ_e on T_e , convective heat flux due to electron density flux, etc.) In the experiments described below, the value of Sh exceeds 5, and the role of convective terms is negligible.

For regimes with Ohmic or central ECR heating at T10, the χ_e^{HP} values (with typical values of order of a 1-3 m^2/s) are usually few times greater than χ_e^{PB} values [1-3] (so-called

“enhanced HPP”). This difference can be explained by dependence of χ_e on ∇T_e [1,3]. The χ_e^{HP} dependence on ∇T_e , however, does not affect the diffusive picture of HPP since it can be written as $\chi_e^{\text{HP}} = \chi_e^{\text{PB}} + (\partial\chi_e^{\text{PB}}/\partial\nabla T_e)\nabla T_e$ (shown analytically and with transport code calculations in [1,3], see also [4] for more references). Moreover, certain calculations were performed for HPP induced by sawteeth oscillations in plasmas with χ_e^{PB} dependent on ∇T_e and $\nabla T_e/T_e$ [1]. The “time-to-peak” (time to reach maximum of δT_e) dependence on radius was almost similar in both cases (with the same initial χ_e^{PB} and same $(\partial\chi_e^{\text{PB}}/\partial\nabla T_e)$ values). This result could be explained by the fact that the value of $sh = |(\delta\nabla T_e/\delta T_e)/(\nabla T_{e0}/T_{e0})|$ was well above 1 (T_{e0} representing background) on the heat wave front and, in this case, $\delta(\nabla T_e/T_e)$ is almost proportional to $\delta\nabla T_e$.

Dependence of χ_e value on $\nabla T_e/T_e$ value when $\nabla T_e/T_e$ exceeds some “critical” level (“critical gradient” model) was highlighted in 1986 for anomalous transport in JET discharges with central heating [7]. This dependence aroused from the so-called “profile consistency” (or “profile stiffness”) which is expressed by a small variation of $\nabla T_e/T_e$ local value with the power increase (or some variation of power profile) observed at many tokamaks (e.g. see [7-9]). Nowadays, the dependences of χ_e^{PB} on the normalized inversed electron temperature gradient length $R/L_{Te} = R\nabla T_e/T_e$ and $\nabla T_e/T_e$ is usually discussed (see [9-10] and references therein). The Ohmic value of R/L_{Te} lies already above the “critical” level because enhanced HPP (induced by sawteeth

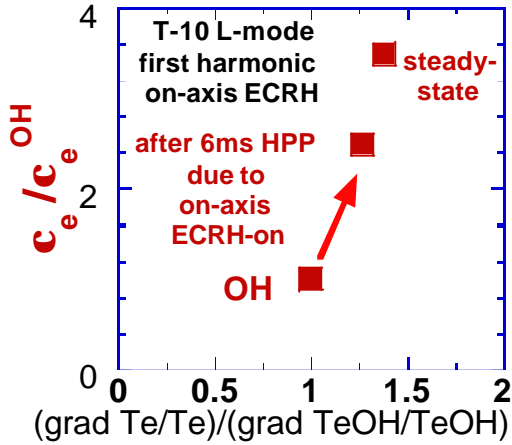


Figure 1. Dependence of c_e/c_{eOH} from $(\tilde{\nabla}T_e/T_e)/\tilde{\nabla}T_{eOH}/T_{eOH}$ at $r/a=0.45$ in 0.17 MA/3T T-10 shot with central ECRH at the first harmonic. c_e data is taken from our successful transport code modelling of steady-states and “enhanced HPP” simultaneously [3].

or on-axis ECRH) is observed at Ohmic background in all tokamaks (e.g. see comparison of T-10 $\chi_{eOH}^{\text{HP}} \approx 0.6-1.2 \text{ m}^2/\text{s}$ at $r/a \sim 0.25-0.45$ with χ_{eOH}^{PB} at T-10 [3]). It is possible to describe the experimental data reported in [3] within various models (e.g. see modelling of experiments [3] with Dnestrovskii canonical profiles model [11]). Moreover, Figure 1 shows the dependence of χ_e/χ_{eOH} on $(\nabla T_e/T_e)/\nabla T_{eOH}/T_{eOH}$ at $r/a=0.45$ in 0.17 MA/3T T-10 shot with central ECRH at the first harmonic [3]. We revisit the results of transport code modelling (with non-linear dependence of the heat flux on ∇T_e) reported by us

in 1987 [3]. The modelling fits well OH and ECRH-heated regimes, sawteeth-induced HPP in OH and ECRH-heated steady-state, and ECRH-induced HPP. An extremely clear strong dependence of χ_e on $\nabla T_e/T_e$ is observed during “enhanced HPP” created by on-axis ECRH switching-on and in new steady-state. In the present report, we focus on cases with $\chi_e^{\text{HP}} < \chi_e^{\text{PB}}$. In T-10, ITB has been recognized by slow and diffusive heat pulse propagation (HPP) induced by central ECRH-onset and slow cold pulse propagation (CPP) by off-axis ECRH cut-off in a sawtooth-free plasma created by off-axis ECRH [2,4,6]. For the first time, this case was observed in T-10 many years ago [2] and called “self-deceleration of heat wave”, or, in a contrast to the L-mode, “reduced” HPP. The diffusive HPP (induced by sawteeth oscillations) across ITB was reported at Alcator C-MOD [12]. Low value of χ_e^{CP} was observed at LHD in the case of CPP inside magnetic island formed by an external perturbation of magnetic field [13].

The presence of internal transport barrier (ITB) means that the anomalous transport almost disappears at best (for example, $\chi_e^{\text{PB}} \approx \chi_i^{\text{PB}} \approx 0.1 \text{ m}^2/\text{s}$ under very high values of $R/L_{Te,i}$ in JT-60U

[14]). Non-local confinement bifurcations (jump of core transport at $\sim 0.3-0.4r/a$ region inside and around ITB in a ms timescale) were observed in various JT-60U normal and RS plasmas and called the ITB-events [5,15]. Later, the ITB-events were found in T-10 plasmas [6]. At the same time, HPP is diffusive between the non-local bifurcations of the transport [5]. Slow outward electron and ion HPP ($\chi_{e,i}^{HP} \sim 0.1 \text{ m}^2/\text{s} \ll \chi_{e,i}$) induced by ITB-event was observed in JT-60U [5]. The process of ITB formation in JT-60U consists from ITB-events and gradual decay of $\chi_{e,i}$ during slow HPP reconstructed in present paper.

2. Interpretation of slow heat (cold) pulse propagation in T-10

Regarding the perturbations of the heat sources, density and convective heat flux, the transport of $\delta T_e(r,t)$ is described by the following full equation :

$$1.5n_e \partial \delta T_e / \partial t = \text{div}(\delta \Gamma_e), \quad \delta \Gamma_e = n_e (\chi_{e0} \nabla \delta T_e + \delta \chi_e (\nabla \delta T_e + \nabla T_{e0})) \quad (3),$$

where χ_{e0} is background power balance electron heat diffusivity, ∇T_{e0} is T_e gradient before HPP, and $\delta \chi_e$ is the variation of power balance electron heat diffusivity during HPP. Comparison of equations (3) and (1) gives follows:

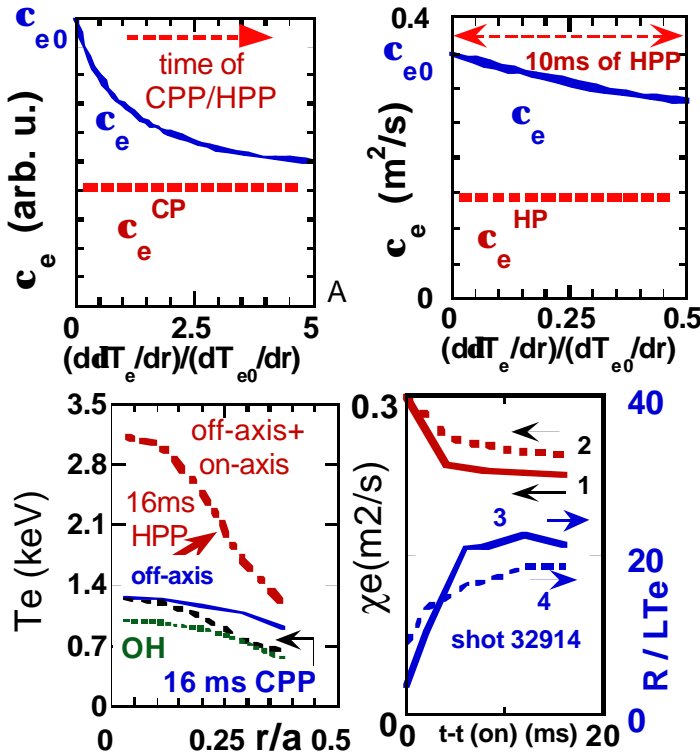
$$n_e \chi_e^{HP} \nabla \delta T_e \approx n_e (\chi_{e0} \nabla \delta T_e + \delta \chi_e (\nabla \delta T_e + \nabla T_{e0})) \quad (4).$$

since calculations with the simplified equation (1) describe experiments at T-10, LHD and JET rather well [1-6,15]). The evolution of $\chi_e \equiv \delta \chi_e + \chi_{e0}$ is described by the following expression derived from eq. (4):

$$\chi_e \approx (\chi_e^{HP} \nabla \delta T_e / \nabla T_{e0} + \chi_{e0}) / (1 + \nabla \delta T_e / \nabla T_{e0}) \quad (5).$$

Fig. (1) shows the dependence of χ_e in eq. (5) which describes diffusive HPP with $\chi_e^{HP} < \chi_{e0}$.

For the first time, slow HPP was found in T-10 nearly 20 years ago [2] in the shots with $I_p=0.38\text{MA}$, $B_t=3\text{T}$, line averaged density $= 4 \cdot 10^{19}/\text{m}^3$. Slow outward HPP with $\chi_e^{HP}=0.14 \text{ m}^2/\text{s}$ at $r/a=0.45$ was created by on-axis ECRH-on (0.36 MW at the first harmonic) imposed on the background sawteeth-free plasmas with 0.9 MW off-axis ECRH started 100ms earlier. The density profile was constant within 15ms after central ECRH-on. The time interval of HPP study was limited to 10ms since the mixture of SXR and ECE data was used in the HPP analysis. Figure 1(c) shows the reconstructed decay of χ_e during HPP at $r/a=0.45$ ($\chi_{e0}=0.35 \text{ m}^2/\text{s}$).



Figures 1 (a-b)

(a) Dependence of c_e on $\tilde{N}dT_e / \tilde{N}dT_{e0}$ (see eq. 5). (b) T-10: Dependence of c_e on $\tilde{N}dT_e / \tilde{N}dT_{e0}$ during outward HPP at $r/a=0.45$ induced by central ECRH-on at the background created by off-axis ECRH [2](first harmonic heating).

Figures 2 (a-b) T-10: (a) T_e profiles at off-axis ECRH (solid line), 16ms after start of on-axis ECRH in shot 32914 (dashed-dotted line), 16 ms after the end of off-axis ECRH in shot 32913 (dashed line) and Ohmic profile (dotted line) (second harmonic ECRH). (b) Evolution of c_e during outward HPP induced by central ECRH-on at the

background created by off-axis ECRH at $r/a=0.24$ (curve 1), $r/a=0.33$ (curve 2). Curves 3 and 4 represents R/L_{Te} measured at same $r/a=0.24$ and 0.33 (see HPP detail in [4]).

In T-10 experiments described in figures 2-3, sawteeth oscillations were suppressed by high-field-side (HFS) off-axis ECRH with 140 GHz (second harmonic) in similar 0.18 MA/ 2.3T shots 32914 and 32913 (see detail of HPP/CPP in [4]). In figure 2(a), the sawteeth-free background is indicated by a solid line. 130 GHz on-axis ECRH imposed on sawteeth-free background creates outward HPP in shot 32914. Dashed-dotted line in Fig. 2(a) shows T_e profile after 16ms of HPP. Figure 2(b) represents the decay of χ_e (see eq. 5) at $r/a=0.24$ (curve 1), $r/a=0.33$ (curve 2). Curves 3 and 4 represents R/L_{Te} measured at same $r/a=0.24$ and 0.33 . The values of R/L_{Te} rises well above OH level (8 and 10) and ITB formation is obvious. χ_e behaves in similar manner in the similar experiments with first harmonic and second harmonic ECRH (year 1989 and 2002).

Off-axis ECRH turn-off creates an inward slow CPP in shot 32913. Dashed line in Fig. 2(a) shows T_e profile after 16ms of CPP. Figure 3(a) represents the evolution of $T_e(r,t)$ during off-axis ECRH. Dotted curves shows calculated timetraces with $\chi_e^{HP}=0.08 \text{ m}^2/\text{s}$ (see detail in [4]). Figure 3(b) shows the evolution of χ_e at $r/a=0.25$ during inward CPP with $\chi_e^{HP}=0.08 \text{ m}^2/\text{s}$ obtained with eq. (5). The values of χ_e obtained from power balance calculations before and at the end of CPP are shown with circles. The reconstructed decay of $\chi_e(t)$ fits well the value of χ_e at the end of CPP (obtained independently from the power balance). Figure 3(c) shows the timetraces of χ_e at $r/a=0.25$ and $r/a=0.16$. At $r/a=0.25$, the value of χ_e falls quickly and R/L_{Te} reaches critical value (OH level) in two ms (R/L_{Te} reaches 17 in the end of CPP). At $r/a=0.16$, the value of χ_e falls slowly and R/L_{Te} reaches critical value only in the middle of CPP. The ITB formation gradually propagates toward the central part of the plasma column and is absent at $r/a < 0.1$.

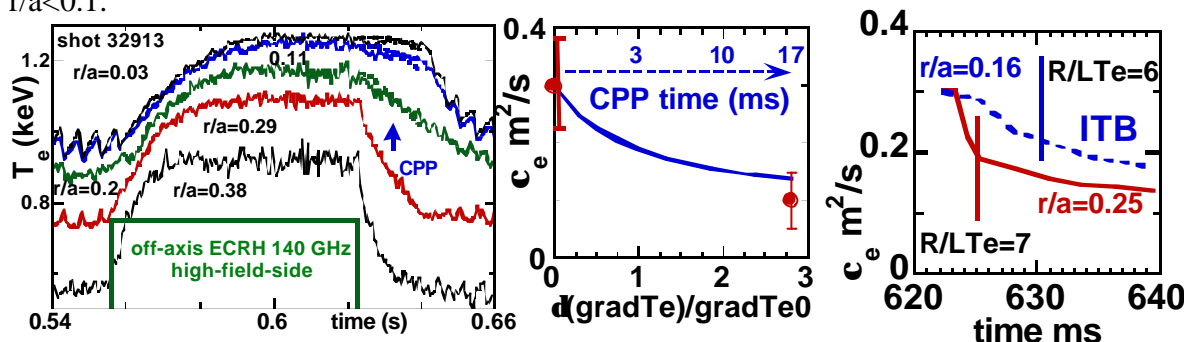


Fig.3 (a-c) T-10: (a) $T_e(r,t)$ evolution during inward CPP from off-axis ECRH cut-off shot 32913. (b) Dependence of c_e on $\tilde{N}dT_e/\tilde{N}T_{e0}$ (obtained from equation (5) at $r/a=0.25$ with $c_e^{HP}=0.08 \text{ m}^2/\text{s}$), circles- power balance values [4].(c) Approximate evolution of c_e at $r/a=0.25$ (R/L_{Te} reaches 17, OH level is 7) and $r/a=0.16$. ITB formation gradually propagates toward the centre.

3. Interpretation of slow electron and ion heat pulse propagation in JT-60U

In JT-60U reverse shear experiments [5-6], ITB-events A and C reduces transport and form stronger ITB. Figures 4(a-b) shows the timetraces of $T_{e,i}$. ITB-event C creates diffusive outward ion and electron HPP with $\chi_e^{HP} \sim 0.1 \text{ m}^2/\text{s}$, $\chi_i^{HP} \sim 0.14 \text{ m}^2/\text{s}$ [5]. Figure 4(c) displays the evolution of toroidal rotation velocity V_t . Figure 5 (a) represents the evolution of χ_e (with two values of χ_{e0}) at $r/a=0.63$ taken from eq. (5). The Power balance calculations were performed using the 1.5 dimensional transport code TOPICS [17]. It is not easy to separate precisely the electron and ion

heat fluxes in the case of NBI heating. The solid curve in Figure 5 represents the evolution of χ_e with the value of χ_{e0} taken from power balance calculations. The dotted line shows the evolution of χ_e with probable lowest limit of $\chi_{e0 \min}$ before the events. In any case, χ_e falls to rather low level of $\sim 0.2\text{-}0.3 \text{ m}^2/\text{s}$. In any case, the χ_e value exceeds $\chi_e^{\text{HP}} \sim 0.1 \text{ m}^2/\text{s}$ value significantly. The value of R/L_{Te} , at $r/a=0.63$ rises up to 27. Figure 6 shows the evolution of χ_i ($r/a=0.7$) with the value of χ_{i0} taken from power balance calculations. The value of R/L_{Ti} , at $r/a=0.7$ rises up to 28. The value of χ_i falls significantly to low enough level $\sim 0.6 \text{ m}^2/\text{s}$. Nevertheless, χ_i value remains high in comparison to the value of $\chi_i^{\text{HP}} \sim 0.14 \text{ m}^2/\text{s}$. The gradual decay of $\chi_{e,i}$ during HPP is accompanied by the rise of ∇P_i and ∇V_t .

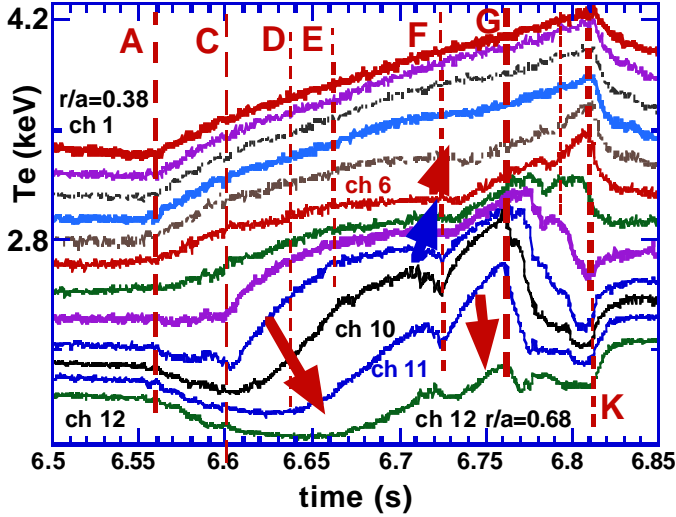


Fig. 4(a-c) JT-60U (a-b) Time-traces of $T_{e,i}$ at ITB-events A, C and outward HPP induced by event C. (c) profiles of toroidal rotation velocity V_t .

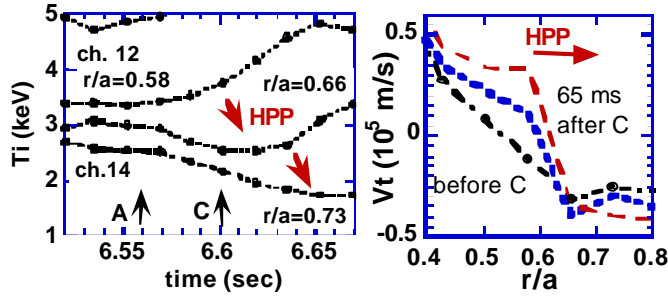


Fig.5 JT-60U- (a) Evolution of c_e (solid line) with the value of c_{e0} taken from power balance calculations and R/L_{Te} at $r/a=0.63$. Dotted line - the evolution of c_e with probable lowest limit of $c_{e0 \min}$ before the events

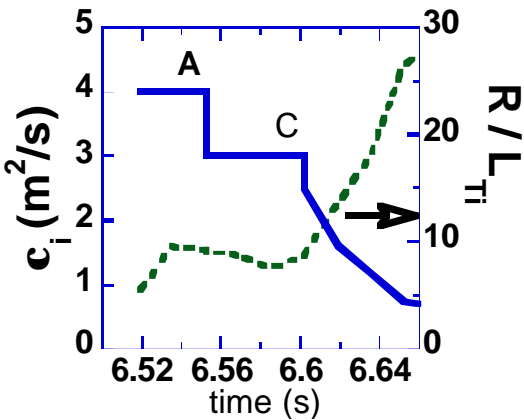


Fig. 6 JT-60U- Evolution of c_i with the value of c_{i0} taken from power balance calculations (solid line) and R/L_{Ti} at $r/a=0.7$. The value of c_i falls significantly to rather low level of $\sim 0.6 \text{ m}^2/\text{s}$. Nevertheless, c_i value remains high in comparison to the value of $c_i^{\text{HP}} \sim 0.14 \text{ m}^2/\text{s}$.

Now we discuss the behaviour of eq. (5) in extreme cases. χ_e decreases almost linearly at small values of $\nabla \delta T_e / \nabla T_{e0}$ since $\chi_e \approx \chi_{e0} - (\chi_{e0} - \chi_e^{\text{HP}}) \nabla \delta T_e / \nabla T_{e0}$ at $\nabla \delta T_e / \nabla T_{e0} \ll 1$. We used this

qualitative explanation of slow HPP during ITB formation earlier [2,4-5]. The opposite case is the interpretation of HPP/CPH experiments with strongly rising T_e gradients ($\nabla\delta T_e / \nabla T_{e0} \gg 1$) on the heat (cold) wave front. In these cases equation (5) may be rewritten as $\lim_{\nabla\delta T_e / \nabla T_{e0} \rightarrow \infty} \chi_e = \chi_e^{\text{HP}}$. (see an obvious limit $\chi_e = \chi_e^{\text{HP}}$ in figure (1)). In this case slow HPP/CPH indeed represents low transport with $\chi_e \approx \chi_e^{\text{HP}}$ in the end of HPP.

If the HPP is absent, i.e. at $\chi_e^{\text{HP}} \approx 0$ [18], the heat wave does not propagate at all, the eq. (5) appears to be an obvious and expected limit:

$$\chi_e = \chi_{e0} / (1 + \nabla\delta T_e / \nabla T_{e0}) \text{ at } \chi_e^{\text{HP}} = 0 \quad (6)$$

Sawtooth-like crash creates outward HPP in RS shot. Profiles of T_e before and after the crash are shown in Fig. 7(a) by solid and dashed curves, respectively. Figure 7(b) shows shifted timetraces of T_e (ch. 9-12). Bold solid and dashed solid lines show calculations of HPP from ch.9 to ch. 11-12 with $\chi_e^{\text{HP}} = 0.1 \text{ m}^2/\text{s}$ (faster as compared with experiment) and with $\chi_e^{\text{HP}} = 0.04 \text{ m}^2/\text{s}$. Heat wave does not propagate at ch. 11 and one cannot obtain χ_e^{HP} value but can only estimate its upper limit $\chi_e^{\text{HP}} < 0.03 \text{ m}^2/\text{s}$. The absence of HPP just represents light decay of χ_e between ch.10 and 11 during $\sim 5 \text{ ms}$ time interval.

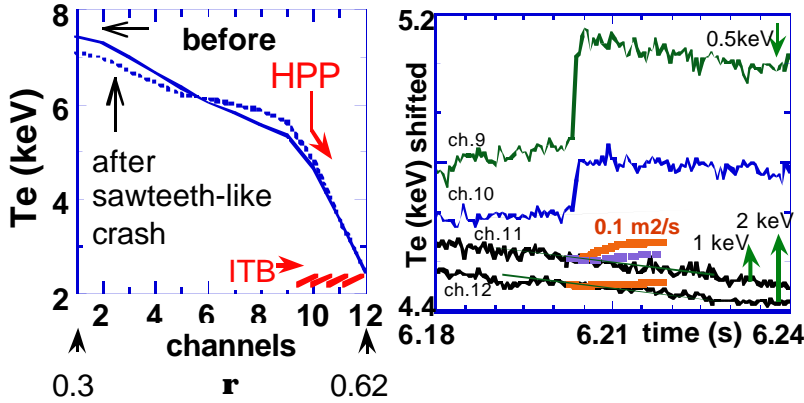


Fig 7(a-b) (a) T_e profiles before and after crash in RS JT-60U shot with NBI and ECRH. (b) Extremely slow HPP (absence of HPP) from ch. 10 to ch. 11,12 (bold solid and dashed lines – calculations with $\chi_e^{\text{HP}} = 0.1 \text{ m}^2/\text{s}$ and $0.04 \text{ m}^2/\text{s}$) See equation 6.

4. Discussion and Conclusions

The heat flux is described by the following expression derived from equation (5):

$$\chi_e \nabla T_e \equiv \chi_e (\nabla T_{e0} + \nabla \delta T_e) \approx \chi_e^{\text{HP}} \nabla T_e + (\chi_{e0} - \chi_e^{\text{HP}}) \nabla T_{e0} \quad (7)$$

$$\text{or } \chi_e \nabla T_e \approx \chi_e^{\text{HP}} \nabla T_e + (\chi_{e0} - \chi_e^{\text{HP}}) \nabla T_{e0} (T_e / T_{e0}) \quad \text{at } \delta T_e / T_{e0} \ll \nabla \delta T_e / \nabla T_{e0} \quad (8).$$

It is almost impossible to choose between equations (7) and (8) since the first term at RHS of equation (8) varies much stronger in comparison with the second term (e.g. at the end of CPP/HPP analysed above, $\delta T_e / T_{e0} = 0.03 \nabla \delta T_e / \nabla T_{e0}$ at JT-60U and $\delta T_e / T_{e0} = 0.07 \nabla \delta T_e / \nabla T_{e0}$ at T-10). The second term is convective term and its presence can be explained by the transport caused by global modes or fluctuations with large radial scale (above $0.2r/a$ in T-10 and $0.1r/a$ in JT-60U).

The new method allows us to reconstruct approximate behaviour of $\chi_{e,i}(r,t)$ during slow electron and ion HPP. In T-10, the reconstructed decay of $\chi_e(t)$ fits well the value of χ_e at the end of CPP (obtained independently from the power balance). The fluctuations level measured by reflectometer [21] falls below the ohmic level in some shots with slow CPP in T-10. In T-10, the dynamic of ITB formation during slow HPP is similar with double frequency ECRH (on-axis ECRH imposed at off-axis ECRH-heated background) at first harmonic (1990 [2]) and the second one [4]. The process of ITB formation in JT-60U consists of the ITB-events and gradual decay of $\chi_{e,i}$ during slow HPP reconstructed in present paper. The values of $\chi_{e,i}$ fall significantly during slow HPP but remain a few times greater in comparison with $\chi_{e,i}^{\text{HP}}$ values (e.g. approximately 0.3 and

0.1 m²/s for electrons, 0.6 and 0.15 m²/s for ions). In J-60U, the gradual decay of $\chi_{e,i}$ during HPP is accompanied by the rise of ∇P_i and ∇V_t (and the rise of the radial electric field E_r shear calculated with neoclassical velocity of the poloidal rotation). In a contrast, calculated E_r just begins to vary slowly after the ITB-event [18]. Nevertheless, the role of E_r is unclear since poloidal rotation measurements are absent.

The authors thank Drs N. Hayashi, Y. Sakamoto, T. Takizuka and many other members of the JT-60U team for fruitful discussions and fine collaboration.

References

- [1] Neudatchin S V 1986 “Influence of Electron Temperature Perturbations on Electron Heat Diffusivity in a Tokamak” in: “Voprosy Atomnoi Nauki i Tekniki” (Questions of Atomic Science and Engineering, Thermonuclear Fusion Series) **3** p 39
- [2] Bagdasarov A. A., Vasin N. L., Neudatchin S. V., Savrukhin P. V. 1991 (Proc. 15th Int. IAEA Conf., Washington, 1990), Vol. **1** (IAEA: Vienna, 1991) 523
- [3] Bagdasarov A A, Vasin N L, Esipchuk Yu V, Neudatchin S V, Razumova K A, Savrukhin P V and Tarasyan K N 1987 Soviet J. Plasma Phys. **13** 517
- [4] Neudatchin S V., Kislov A. Ya, Krupin V. A. et al 2003 Nucl. Fusion **43** 1405
- [5] Neudatchin S V, Takizuka T, et al Plasma Phys. Contr. Fusion 1999 **41** L39 and 2001 **43** 661
- [6] Neudatchin S V., Inagaki S, Itoh K., et al. 2004 J. Pl. and Fus. Res. Series **6** 134
- [7] Rebut P. et al 1987 Proc. 11th Int. Conf. on Plasma Physics and Controlled Fusion Research (Kyoto, 1986) vol 2, (Vienna: IAEA) p 187
- [8] AlikaeV V. V. et al., 1988 Sov. J. Plasma Phys. **14** 601
- [9] Ryter F., et al 2001 Nuclear Fusion **41** 537
- [10] Tardini G., Peeters A.G., Pereversev G. V., et al, 2002 Nuclear Fusion, **42**, L11
- [11] Dnestrovskii Yu. N. et al, 1988 19th EPS Conf. on Contr. Fus. and Pl. Ph. (Dubrovnik)
- [12] Wukitch S J *et al* 2002 *Phys. Plasmas* **9** 2149
- [13] Inagaki S *et al* 2004 *Phys. Rev. Lett.* **92** 55002
- [14] Shirai H, et al 1999 Nucl. Fusion **39** 1713
- [15] Neudatchin S V, Takizuka T, Hayashi H, et al, 2004 Nucl. Fusion **44** 945
- [16] Neudatchin S V, Cordey J G and Muir D J 1993 20th EPS Conf. on Contr. Fus. and Plasma Ph. (Lisboa,) vol.I (EPS), p 83
- [17] Shirai H, Takizuka T, Koide Y et al 2000 Plasma Phys. Control. Fusion **42** 1193
- [18] Neudatchin S V, Takizuka T, et al 2006 Fusion Energy (Proc 20th IAEA Fusion Energy Conf. Cnengdo 2006) EXP1/08
- [19] Joffrin E., Alper B, Challis C.D. et al 2000 27th EPS Conf. on Contr. Fus. and Pl. Ph. (Budapest) ECA vol 24B p 237
- [20] Neudatchin S V, Takizuka T, Shirai H, et al Proc. 18th IAEA Fusion Energy Conf. on Fusion Energy (Sorrento, 2000) (Vienna: IAEA)CR-ROM file EXP5/01
- [21] Vershkov V.A. *et al*, 2005 *Nucl. Fusion* **45** S203